Methods for reconstruction of optical parameters from the data of sounding of the atmosphere by a polarization lidar. Part 1. Problems of *a priori* uncertainty in calibration of signals and solutions

S.V. Samoilova

Institute of Atmospheric Optics,
Siberian Branch of the Russian Academy of Sciences, Tomsk

Methods for interpretation of polarization lidar measurements are considered. Prominence is given to selection of an optimal algorithm for calibration of solution, in particular, against a significant multiple scattering background. Two methods for retrieving the profile of the aerosol depolarization ratio from polarization components of a lidar signal are described. The peculiarities of the methods in interpretation of signal profiles obtained from ground-based sensing are analyzed.

Introduction

Lidar polarization measurements are very informative means of remote sensing of the atmosphere, as they are sensitive to the shape and orientation of aerosol particles.[1] As known, the state of light polarization is described by the set of four Stokes parameters, and the scattering properties of the medium are described by the scattering phase matrix. Hence, the aim of polarization measurements could be the determination of the Stokes parameters of backscattered radiation (see, for example, Refs. 1 and 2) or determination of some elements of the scattering phase matrix.[3]

The so-called depolarization ratio δ that is defined by combination of some elements of the scattering phase matrix and depends on the particle shape is usually determined in the simplest variant of polarization measurements. It is known that for spherical particles $\delta = 0$ if scattering has occurred exactly backwards and only single scattering took place. On the contrary, radiation backscattered from non-spherical particles is to a certain extent depolarized. Depolarization is usually observed when the particles are chaotically oriented. However, some caution is needed when interpreting polarization measurements, because depolarization of radiation can also occur in an aerosol medium consisting of spherical particles under conditions of multiple scattering[4] and it may be absent for non-spherical particles the size of which is comparable with the wavelength of incident radiation.[5]

Principal attention in the first part of the paper is paid to the methods used for retrieval of the backscattering coefficients and depolarization ratio with a correction made for the contribution due to molecular scattering. The algorithm for inverting the polarized components of lidar returns applicable in the absence of data on the sensitivity ratio between the polarization channels is considered. Possible errors in setting the boundary values are studied (the so-called methods of local or integral calibration), including the case of the presence of significant background due to multiple scattering.

1. Model of the lidar equation (single scattering approximation)

In the case of a long sounding path, the backscattered signal, at the output of a photodetector, is described by the lidar equation. In the single scattering approximation for linearly polarized radiation it can be written in the form[6,7]:

$$F_i(z) = \frac{P_i}{z^2} T^2(z_0, z)\sigma(z)\mathbf{K}_i A(z)\mathbf{S}^{(0)}, \quad i=\perp, \parallel \quad (1)$$

where the signs "$\parallel$" and "$\perp$" denote parallel and perpendicular components of the parameters; P is the instrumentation constant taking into account transmission of the optics and sensitivity of the photodetector in the ith channel, σ is the extinction coefficient,

$$T^2(z_0, z) = \exp\left\{-2\int_{z_0}^{z}\sigma(z')\mathrm{d}z'\right\};$$

is the total transmission, $\mathbf{K}_i$ is the instrumentation vector, A is the normalized scattering phase matrix, $\mathbf{S}^{(0)}$ is the Stokes vector-parameter of radiation normalized to its intensity. The instrumentation vector is the first row of the Mueller matrix describing the effect of optical elements of the receiving part of the lidar on the Stokes parameters of received radiation; for a polarizer

$$\mathbf{K}_1 = \frac{1}{2}(1 \quad 1 \quad 0 \quad 0), \quad \mathbf{K}_2 = \frac{1}{2}(1 \quad -1 \quad 0 \quad 0).$$

Let us assume that the scattering phase matrix in the problem under consideration has the form:

$$A_{ij} = \begin{pmatrix} a_{11} & a_{12} & 0 & 0 \\ a_{12} & a_{22} & 0 & 0 \\ 0 & 0 & a_{33} & -a_{43} \\ 0 & 0 & a_{43} & a_{44} \end{pmatrix}.$$

This assumption is correct both for liquid droplet clouds[8] under condition that $a_{33} = a_{44}$, $a_{12} = 0$ and for crystal clouds comprising symmetric particles of one and the same type chaotically orientated in space.[9] Let us consider the case of linearly polarized sounding radiation. Let us choose the coordinate system so that the state of polarization of sounding radiation is described by the Stokes vector-parameter

$$\mathbf{S}^{(0)} = \begin{pmatrix} 1 \\ 1 \\ 0 \\ 0 \end{pmatrix}.$$

Then formulas (1) can be written in the following form

$$F_i(z) = \frac{P_i}{z^2}\beta_i(z)T^2(z_0,z), \quad i = \perp, \parallel$$

where

$$\beta_\parallel(z) = \beta(z)S(z)\frac{1}{2}\big[a_{11}(z) + 2a_{12}(z) + a_{22}(z)\big];$$

$$\beta_\perp(z) = \beta(z)S(z)\frac{1}{2}\big[a_{11}(z) - a_{22}(z)\big];$$

and

$$\beta(z) = \beta_\parallel(z) + \beta_\perp(z)$$

is the total backscattering coefficient,

$$S(z) = \sigma(z)/\beta(z)$$

is the lidar ratio.

For an aerosol−gas medium

$$\beta_\parallel = \beta_{a,\parallel} + \beta_{m,\parallel} \quad \text{and} \quad \beta_\perp = \beta_{a,\perp} + \beta_{m,\perp},$$

where the subscripts "a" and "m", respectively, denote the contributions of aerosol (including clouds) and molecular components of the atmosphere. One can assume that the molecular depolarization ratio $\delta_m = \beta_{m,\perp}/\beta_m$, and the lidar ratio $S_m = \sigma_m/\beta_m = 8\pi/3$ in the atmosphere are constant. The correct determination of the aerosol depolarization ratio

$$\delta_a = \beta_{a,\perp}/\beta_{a,\parallel} = (a_{11} - a_{22})/(a_{11} + 2a_{12} + a_{22})$$

is the primary purpose of interpretation of lidar polarization measurements and, together with estimation of the lidar ratio

$$S_a = \sigma_a/\beta_a = (a_{11} + a_{12})^{-1},$$

it often enables one to identify the type and shape of aerosol particles.

The lidar equations (1) for a two-component medium can be rewritten in the form

$$F_i(z) = \frac{P_i}{z^2}\big[\beta_m(z)C_{m,i} + \beta_a(z)C_{a,i}\big]T_m^2(z_0,z)T_a^2(z_0,z),$$

$$i = \perp, \parallel \qquad (2)$$

where

$$C_{a,\perp} = \frac{\delta_a}{1+\delta_a}, \quad C_{m,\perp} = \frac{\delta_m}{1+\delta_m},$$

$$C_{a,\parallel} = \frac{1}{1+\delta_a}, \quad C_{m,\parallel} = \frac{1}{1+\delta_m}. \qquad (3)$$

In the single scattering approximation the polarized components of the lidar signal are related to the Stokes vector components by the following relationships:

$$\mathbf{S}^{(1)}(z) = \begin{pmatrix} F_\parallel(z)/P_\parallel + F_\perp(z)/P_\perp \\ F_\parallel(z)/P_\parallel - F_\perp(z)/P_\perp \\ 0 \\ 0 \end{pmatrix} =$$

$$= \begin{pmatrix} \big[\beta_m(z)C_{m,1}(z) + \beta_a(z)C_{a,1}(z)\big]T_m^2(z_0,z)T_a^2(z_0,z)/z^2 \\ \big[\beta_m(z)C_{m,2}(z) + \beta_a(z)C_{a,2}(z)\big]T_m^2(z_0,z)T_a^2(z_0,z)/z^2 \\ 0 \\ 0 \end{pmatrix},$$

$$(4)$$

where

$$C_{a,1} = 1, \; C_{m,1} = 1, \; C_{a,2} = \frac{1-\delta_a}{1+\delta_a}, \; C_{m,2} = \frac{1-\delta_m}{1+\delta_m}. \quad (5)$$

2. Methods of inverting the lidar equation (single scattering approximation)

A. Local calibration

The aerosol depolarization ratio δ_a of a two-component medium is related to the components of the scattering phase matrix and the optical characteristics by the following relationship[10]:

$$\delta_a = \frac{\beta_{a,\perp}}{\beta_{a,\parallel}} = \frac{a_{11} - a_{22}}{a_{11} + 2a_{12} + a_{22}} = \frac{R\delta(\delta_m+1) - \delta_m(\delta+1)}{R(\delta_m+1) - (\delta+1)}, \quad (6)$$

where $R = (\beta_m + \beta_a)/\beta_m$ is the scattering ratio, and δ is the total depolarization ratio. The depolarization coefficient δ_a can be obtained from Eq. (4) if $R(z)$ has been preliminary determined, or directly from Eq. (1) by reconstructing $\beta_{a,\parallel}$ and $\beta_{a,\perp}$. In the former case it is necessary to know the sensitivity ratio between the polarization channels $P_\parallel/P_\perp$ (see the methods of instrumentation calibration in Ref. 7) in order to correctly determine $\delta = \beta_\perp/\beta_\parallel = (P_\parallel F_\perp)/(P_\perp F_\parallel)$ (let us note that the latter equality is correct only in the single scattering approximation). Let us consider the second case in a more detail.

To invert Eq. (2) let us multiply its left and right parts by

$$z^2 \exp\left\{2\left[S_m - C_{m,i}S_a / C_{a,i}\right] \int_{z_0}^{z} \beta_m(z')\mathrm{d}z'\right\}$$

and then we obtain the formulas for the polarized components of the backscattering coefficient:

$$\psi_i(z) = P_i\beta_i(z)\exp\left\{-2S_a / C_{a,i} \int_{z_0}^{z} \beta_i(z')\mathrm{d}z'\right\},$$

where

$$\psi_i(z) = F_i(z)z^2 \exp\left\{2\left[S_m - \frac{C_{m,i}}{C_{a,i}}S_a\right] \int_{z_0}^{z} \beta_m(z')\mathrm{d}z'\right\},$$

$$i = \perp, \parallel. \tag{7}$$

These can be transformed to Bernoulli equation by taking the logarithm and differentiating

$$\beta_i'(z) - \beta_i(z)\left[\ln\{\psi_i(z)\}\right]' = \frac{2S_a}{C_{a,i}}\beta_i^2(z),$$

The stable solutions of this equation, similarly to Refs. 11 and 12, have the form

$$\beta_i(z) = \frac{\psi_i(z)}{\dfrac{\psi_i(z_*)}{C_{m,i}\beta_m(z_*) + C_{a,i}\beta_a(z_*)} - \dfrac{2S_a}{C_{a,i}}\displaystyle\int_{z}^{z_*}\psi_i(z')\mathrm{d}z'}. \tag{8}$$

Let us note that the equations for the Stokes vector components (4) can be inverted in analogous way if assuming that

$$\psi_i(z) = S_i(z)z^2 \exp\left\{2\left[S_m - \frac{C_{m,i}}{C_{a,i}}S_a\right] \int_{z_0}^{z} \beta_m(z')\mathrm{d}z'\right\},$$

$$i = 1, 2. \tag{9}$$

As the sought value of δ_a stands in Eq. (8) in explicit form, let us apply the iteration procedure:

1) $\delta_a^{(0)} \in \,]0, 1[\,$ is set;

2) the constants and functions entering Eq. (8) are determined according to Eqs. (3) and (7) and $\beta_{a,\perp}^{(i)}$, $\beta_{a,\parallel}^{(i)}$ are reconstructed;

3) $\delta_a^{(i)} = \beta_{a,\perp}^{(i)} / \beta_{a,\parallel}^{(i)}$ is calculated, and then the steps 2 and 3 are repeated.

Calculations have shown stability of the procedure to the initial approximation. Fulfillment of the condition $|\delta_a^{(i)} - \delta_a^{(i-1)}| < \varepsilon$ can be a criterion of convergence of iterations.

The algorithms for reconstructing of the optical parameters were examined using the data of sounding by means of the polarization lidar at the Institute for Tropospheric Research (Leipzig, Germany). The measurements with the Raman channel in this lidar enables us to retrieve the backscattering coefficient taking into account inhomogeneity of the lidar ratio along the sounding path and to use the obtained profile as the standard in comparing the results.[13,14] Sounding was performed during 35 minutes (71 realizations, each of which was obtained by summing of 9000 shots) at the wavelengths of $\lambda_0 = 532$ nm in the aerosol polarization channels (the sensitivity ratio is known) and at $\lambda_R = 607$ nm in the Raman channel. Profiles of the molecular components were calculated by the standard formula using known values of temperature and pressure.

Figure 1 shows the results of comparison of different methods (local calibration) for reconstruction of the aerosol backscattering coefficient, aerosol depolarization ratio, and scattering ratio from the data obtained on November 29, 1999, the beginning of measurements was at 3:51 p.m. Let us note that the accuracies of reconstruction of the cloud parameters using all three algorithms practically coincide, the presence of oscillations of the aerosol part of the profile $\delta_a(z)$ above the cloud is explained by the fact that reconstruction of $\delta_a(z)$ is unstable at $R(z) < 1.1$ (Ref. 10).

The lidar ratio profile was reconstructed from the data of sounding by a Raman lidar (the applied method is described in Ref. 15). The value S_a used in Eq. (8) here and below is set constant along the sounding path and equal to 30 sr, that corresponds to the mean value S_a in a cloud (according to the estimates for the purely aerosol parts, $S_a = 55$ sr). Inconstancy of the lidar ratio doest not essentially affect the accuracy of reconstruction of the optical parameters, at least, in the considered case. In the general case, the problem of *a priori* uncertainty in setting the lidar ratio when interpreting the data of single-frequency sounding can not be solved, one can estimate its mean value and the rate in a cloud,[14,16] but the only possible way for the cloudless atmosphere is the use of the relevant models.[17]

In addition to inconstancy of the lidar ratio, the error in setting the boundary conditions (first term in the denominator of Eq. (8)) essentially affects the accuracy of reconstruction of the parameters. Local calibration at the end of the sounding path ($z_* = 18$ km) and the assumption that $\beta_m(z_*) + \beta_a(z_*) \cong$

$\cong \beta_m(z_*)$ were used for obtaining the results shown in the left part of Fig. 1. This assumption can also be used for calibration at a point below the cloud ($z_* = 8$ km, right part of Fig. 1), however, the accuracy of reconstruction of the optical parameters is lower, especially as concerning the aerosol parts.

Reconstruction of the depolarization coefficient is also unstable, especially at the lower boundary of clouds. Nevertheless, one can consider the results satisfactory. As will be shown below, expediency of the local calibration below the cloud is justified in the presence of the multiple scattering.
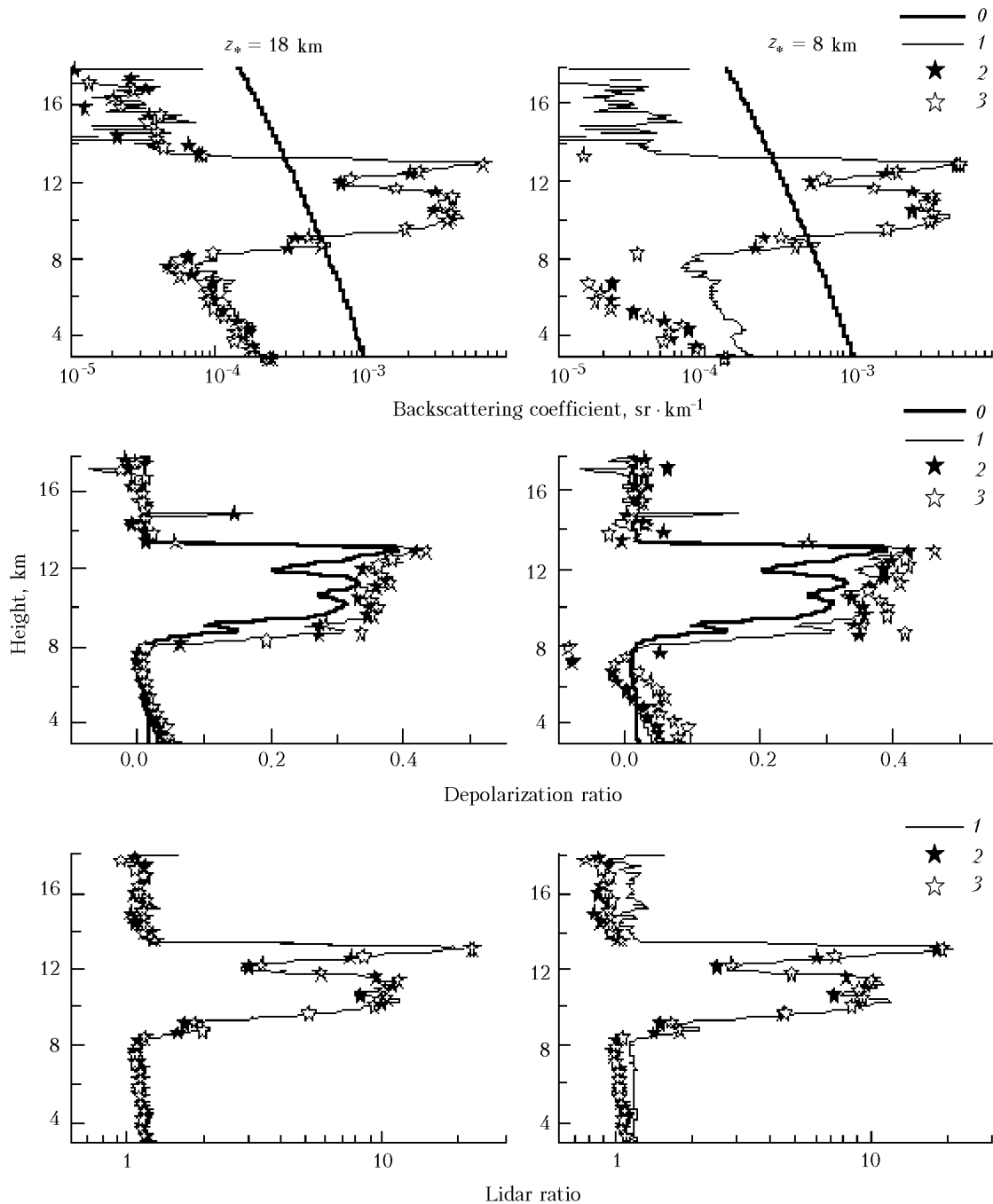
Fig. 1. Comparison of different methods for reconstruction of the optical parameters (local calibration): curves *1* are used as a standards, curves *2* are obtained according to Eqs. (8) and (9) at inversion of the equations for the Stokes vector components (4) (the sensitivity ratio of the polarization channels is assumed to be known), curves *3* are the same at inversion of the lidar equations (2) according to Eqs. (7) and (8) and unknown sensitivity of the channels. Curve *0* in Fig. 1*a* shows the profile of the molecular backscattering coefficient, curve *0* in Fig. 1*b* shows the total depolarization ratio.

B. Integral calibration

If lidar measurements have been carried out in the daytime, or the lidar has been placed significantly far from the object of sounding (spaceborne sounding), significant sky light background is certainly present in the signal (for example, the signal in LITE measurements,[18] orbit 79, September 1994, 7:15 p.m. UTC is only 20% of the total signal[19]). The absence of signal from aerosol can be observed both below and above the cloud, and in this case, it is more expedient to use the so-called integral calibration[20] and to estimate the calibration parameters directly from the lidar returns. The following formula is correct for a two-component medium in inverting the signals relative to the polarized components of the backscattering coefficient:

$$\beta_i(z) = \frac{\psi_i(z)}{\left[\dfrac{2S_a}{C_{a,i}}\displaystyle\int_{z_0}^{z*}\psi_i(z')dz'/(1-V_{*,i}^2)\right] - \dfrac{2S_a}{C_{a,i}}\displaystyle\int_{z}^{z*}\psi_i(z')dz'},$$

$$i = \perp, \parallel \text{ or } 1,2, \tag{10}$$

where

$$V_{*,i}^2 = T_a^2(z_0,z_*)\exp\left\{-2\int_{z_0}^{z*}\frac{S_a C_{m,i}}{S_m C_{a,i}}\sigma_m(z')dz'\right\}. \tag{11}$$

The relationships for $\psi_i(z)$, $C_{a,i}$, and $C_{m,i}$ are analogous to that presented in Eqs. (3), (5), (7), (9). The first factor in Eq. (8) is unknown for calibration. If there was a signal below and above the cloud, $T_c^2(z_1, z_2)$, where z_1 and z_2, respectively, are the lower and upper boundaries of the cloud, then, according to Eqs. (10), (11) and replacing z_0 and z_1 with z_* and z_2, one can estimate and reconstruct[16] $\beta_{c,i}(z)$, the profile of backscattering coefficient in the cloud. The following procedure can be applied to reconstruction of the entire profile.

Let us set the family of solutions $\beta_i(z, \alpha)$ depending on the parameter α:

$$\beta_i(z, \alpha) =$$

$$= \frac{\psi_i(z)}{\left\{\dfrac{2S_a}{C_{a,i}}\displaystyle\int_{z_0}^{z*}\psi_i(z')dz'/[1-V_{*,i}^2(\alpha)]\right\} - \dfrac{2S_a}{C_{a,i}}\displaystyle\int_{z}^{z*}\psi_i(z')dz'},$$

$$i = \perp, \parallel \text{ or } 1,2, \tag{12}$$

where

$$V_{*,i}^2(\alpha) = \alpha\exp\left\{-2\int_{z_0}^{z*}\frac{S_a C_{m,i}}{S_m C_{a,i}}\sigma_m(z')dz'\right\}. \tag{13}$$

Obviously, the value α at which $\beta_i(z, \alpha)$ coincides with the exact solution of Eqs. (2) and (4) is the sought estimate of $T_a^2(z_0, z_*)$, and, to determine α, it is sufficient to minimize the functional

$$\Phi_\alpha = \int_{z_1}^{z_2}(\beta_{c,i}(z) - \beta_{a,i}(z,\alpha))^2 dz. \tag{14}$$

It is worth using the method of integral calibration Eqs. (10), (11) in the presence of accompanying photometric measurements of the atmospheric transmission.[21] The case when signal outside a cloud is absent and no additional measurements available is most difficult for interpretation. Then it seems reasonable to preliminary estimate $\beta_{c,i}(z)$ by either the method of asymptotic signal or by the method of logarithmic derivative with subsequent correction for the solution according to Eqs. (12)–(14) (this procedure for a single-component medium is described in detail in Ref. 19).

Figure 2 shows the comparison of two methods (integral calibration) for reconstruction of the aerosol backscattering coefficient, aerosol depolarization ratio, and scattering ratio from the data obtained by polarization lidar on November 29, 1999. Left column corresponds to the profiles reconstructed with the estimation of $T_c^2(z_1,z_2)$ according to Ref. 16 and the right column corresponds to the profiles reconstructed under conditions of complete *a priori* uncertainty with the estimation of $\beta_i(z)$ by the method of asymptotic signal

$$\beta_i(z) = \frac{\psi_i(z)}{\dfrac{2S_a}{C_{a,i}}\displaystyle\int_{z}^{z_{max}}\psi_i(z')dz'}$$

with subsequent correction of the solution according to Eqs. (12)–(14).

Analysis of the results shows that the accuracies of reconstruction of the parameters of cloud by all three methods practically coincide with each other, what confirms the possibility of independently interpreting the polarized components of the lidar return under conditions of *a priori* uncertainty. The errors in reconstruction of aerosol parts essentially depend on the errors in setting the boundary conditions, but they are higher as compared with the methods of local calibration (see Fig. 1). The latter enables one to give preferences to the methods of local calibration, if, saying again, the data on aerosol signals is available, and additional measurements (for example, photometric) are absent.

3. Model of the lidar equation (multiple scattering approximation)

One more factor, which should be taken into account when interpreting polarization measurements, is the contribution of multiple scattering (MS). This contribution to the total signal is small for the majority of ground-based lidar systems, and one can take into account its effect using, similar to Refs. 22 and 23, the following model of the Stokes vector components:

$$\mathbf{S}(z) = \begin{pmatrix} F(z)/P + F_\perp(z)/P_\perp \\ F(z)/P - F_\perp(z)/P_\perp \\ 0 \\ 0 \end{pmatrix} =$$

$$= \begin{pmatrix} [\beta(z) + \beta_\perp(z)]T_m^2(z_0,z)\exp\left\{-2\int_{z_0}^z \eta_1(z')\sigma_a(z')dz'\right\}/z^2 \\ [\beta(z) - \beta_\perp(z)]T_m^2(z_0,z)\exp\left\{-2\int_{z_0}^z \eta_2(z')\sigma_a(z')dz'\right\}/z^2 \\ 0 \\ 0 \end{pmatrix},$$

$$(15)$$

where

$$\eta_1(z) = 1 - \frac{\ln\left\{S_1(z)/S_1^1(z)\right\}}{2\tau(z)} \approx \text{const},$$

$$\eta_2(z) = 1 - \frac{\ln\left\{S_2(z)/S_2^1(z)\right\}}{2\tau(z)} \approx \text{const}.$$

Then the return signals for linear polarization are described by the formulas:

$$F_\perp(z) = \frac{S_1(z) - S_2(z)}{2} =$$

$$= \frac{\beta_\perp(z)T_m^2(z_0,z)}{z^2} \frac{\exp\left\{-2\eta_1(z)\tau_a(z)\right\} + \exp\left\{-2\eta_2(z)\tau_a(z)\right\}}{2} +$$

$$+ \frac{\beta(z)T_m^2(z_0,z)}{z^2} \frac{\exp\left\{-2\eta_1(z)\tau_a(z)\right\} - \exp\left\{-2\eta_2(z)\tau_a(z)\right\}}{2},$$
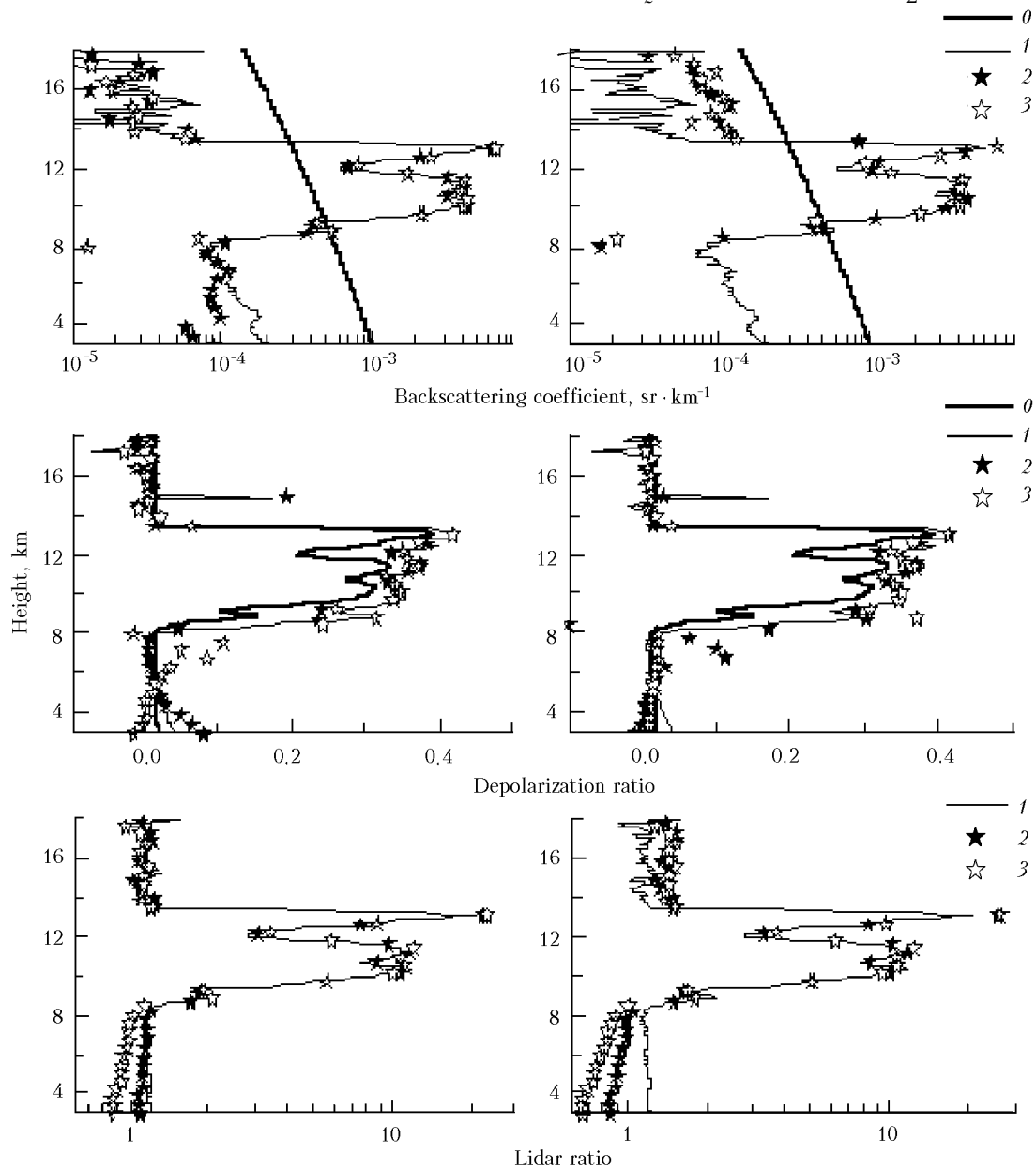

Fig. 2. The same as in Fig. 1 for integral calibration. Left part of the figures is obtained at estimation of $T_c^2(z_1, z_2)$ according to Ref. 16, right part is obtained at adaptive estimation of $T_c^2(z_1, z_2)$ from lidar returns.

$$F(z) = \frac{S_1(z) + S_2(z)}{2} =$$

$$= \frac{\beta(z)T_m^2(z_0,z)}{z^2} \frac{\exp\{-2\eta_1(z)\tau_a(z)\} + \exp\{-2\eta_2(z)\tau_a(z)\}}{2} +$$

$$+ \frac{\beta_\perp(z)T_m^2(z_0,z)}{z^2} \frac{\exp\{-2\eta_1(z)\tau_a(z)\} - \exp\{-2\eta_2(z)\tau_a(z)\}}{2}.$$

$$(16)$$

In the general case, η_1 and η_2 do not coincide for different types of scatterers, and one cannot formally invert Eq. (16) by the methods described in Section 1. However, as the values η_1 and η_2 are close to each other, below we will examine the possibility of using the model

$$F_i(z) = \frac{P_i\beta_i(z)T_m^2(z_0,z)}{z^2}\exp\{-2\eta_i(z)\tau_a(z)\}, \quad i = \perp, \parallel \quad (17)$$

(it is important that $\eta_{\perp,\parallel}$ do not necessarily coincide with $\eta_{1,2}$). Then let us consider possible errors in reconstructing the parameters in the presence of multiple scattering and the effect of the condition $\eta_1 \neq \eta_2$ on the choice of the calibration method for inverting Eqs. (15) and (17).

4. Methods of inverting the lidar equation (multiple scattering approximation)

The possibility of using the models (15) of the Stokes vector components and (17) of the polarized components of the lidar signal enables one to easily transform Eqs. (8) and (10) and to reconstruct the optical parameters taking into account the MS contribution. By replacing in Eqs. (8) and (10), S_a for $S_{a,i} = S_a\eta_i$ ($i = \perp, \parallel$ or 1,2) we obtain the profiles of the polarized components of the backscattering coefficient that obey the relationships (15) and (17).

The following procedure for modeling the lidar returns was realized for examination of the efficiency of the methods in the presence of a significant MS background. The measurement data used for interpretation in Section 2, were taken as the signals caused by single scattering. The multiple scattering disturbance was superposed on the Stokes vector components at $\eta_1 = 0.5$ and $\eta_2 = 0.6$ (MS from aerosol was not taken into account) using the extinction coefficient profile reconstructed from the data of Raman channel. Then $F_\parallel$ and $F_\perp$ was calculated by Eq. (16). Figures 3 and 4 show the results of comparison of different methods for reconstruction of the aerosol backscattering coefficient, aerosol depolarization ratio, and scattering ratio from the model signals calculated according to the procedure described above. Curves 1 are used as the standard for examination of the algorithms. They are obtained using the Raman channel in the single scattering approximation.

Curves 2 are obtained according to Eqs. (8) and (10) at inversion of the equations for the Stokes vector components (15) (the sensitivity ratio between the polarization channels is assumed to be known), curves 3 show the same at inversion of the lidar equations (17) according to Eqs. (8) and (10) and unknown sensitivity of the channels.

Figure 3 shows the reconstruction of the parameters without a correction for the MS background. The method of local calibration (7) and (8) was used for calculations at $z_* = 18$ km (left part of Fig. 3) and $z_* = 8$ km (right part of Fig. 3) assuming that

$$\beta_m(z_*) + \beta_a(z_*) \cong \beta_m(z_*).$$

Obviously, the presence of the MS background affects the accuracy of reconstruction of all parameters (compare the results shown in Fig. 1) that leads to underestimating the values of the aerosol backscattering coefficient and the scattering ratio and overestimating the aerosol depolarization ratio. The choice of the calibration point behind the upper boundary of the cloud, valid from the standpoint of stability of the results obtained, is not good, because the profile is completely destroyed when reconstructing $\delta_a(z)$ from $F_\parallel$ and $F_\perp$, and it leads to significant errors in aerosol parts in reconstructing $\beta_a(z)$. Let us note that adequate reconstruction results are obtained in inverting the signals at $\eta_1 = \eta_2$ and coinciding models (16) and (17). We do not present the data here, because the assumption $\eta_1 = \eta_2$ is not fulfilled for different scattering phase matrices (we will consider this issue in details in the second part of the paper). At the same time, at calibration below a cloud where no effect of MS occurs, the valid results are obtained by any method of reconstruction. The exceptions are the overestimated values of all parameters behind the upper boundary of the cloud. The MS background has more destroying influence on the accuracy of determination of the profiles by the method of integral calibration (10), because, according to Eq. (11), $S_{a,i} = S_a\eta_i$ is involved into the calibration parameter in explicit form, and the results are unstable when using any method of reconstruction. Application of the integral calibration is justified only if a correction for the MS background is done simultaneously with correction of $V_{*,i}^2$. It necessarily should be taken into account if accompanying measurements are used.[21]

Figure 4 shows the results of reconstruction of the parameters with a correction for the MS background at known η_1 and η_2 (the values $\eta_\perp = \eta_\parallel = \eta_1 = 0.5$ were set for processing the signals $F_\parallel$ and $F_\perp$). The profiles reconstructed by the method of local calibration ($z_* = 8$ km) are shown in the left part of the figure. The profiles reconstructed by the method of integral calibration with the estimation of $T_c^2(z_1, z_2)$ according to Ref. 16 and subsequent correction of the solution by the algorithm (12)–(14)

are shown in the right part of the figure. Analysis of the results shows that the accuracies of reconstruction of the parameters on cloud part by all three methods practically coincide with each other and are comparable with the accuracy of reconstruction in the absence of the MS background. Reconstruction on aerosol parts by the method of integral calibration is less stable, but practically coincides at inversion of the Stokes vector components and at inversion of $F_\parallel$ and $F_\perp$.

The results presented in Figs. 3 and 4 show the possibility of independently interpreting the polarized components of the lidar signals and applicability of the model (17) at $\eta_1 \neq \eta_2$. In the second part we will consider in detail the features of variability of $\eta_1(z)$ and $\eta_2(z)$ for different types of scattering particles and different geometry of sounding (including the spaceborne lidar), as well as the methods for estimation of the MS contribution for achieving an adequate reconstruction of the optical parameters.
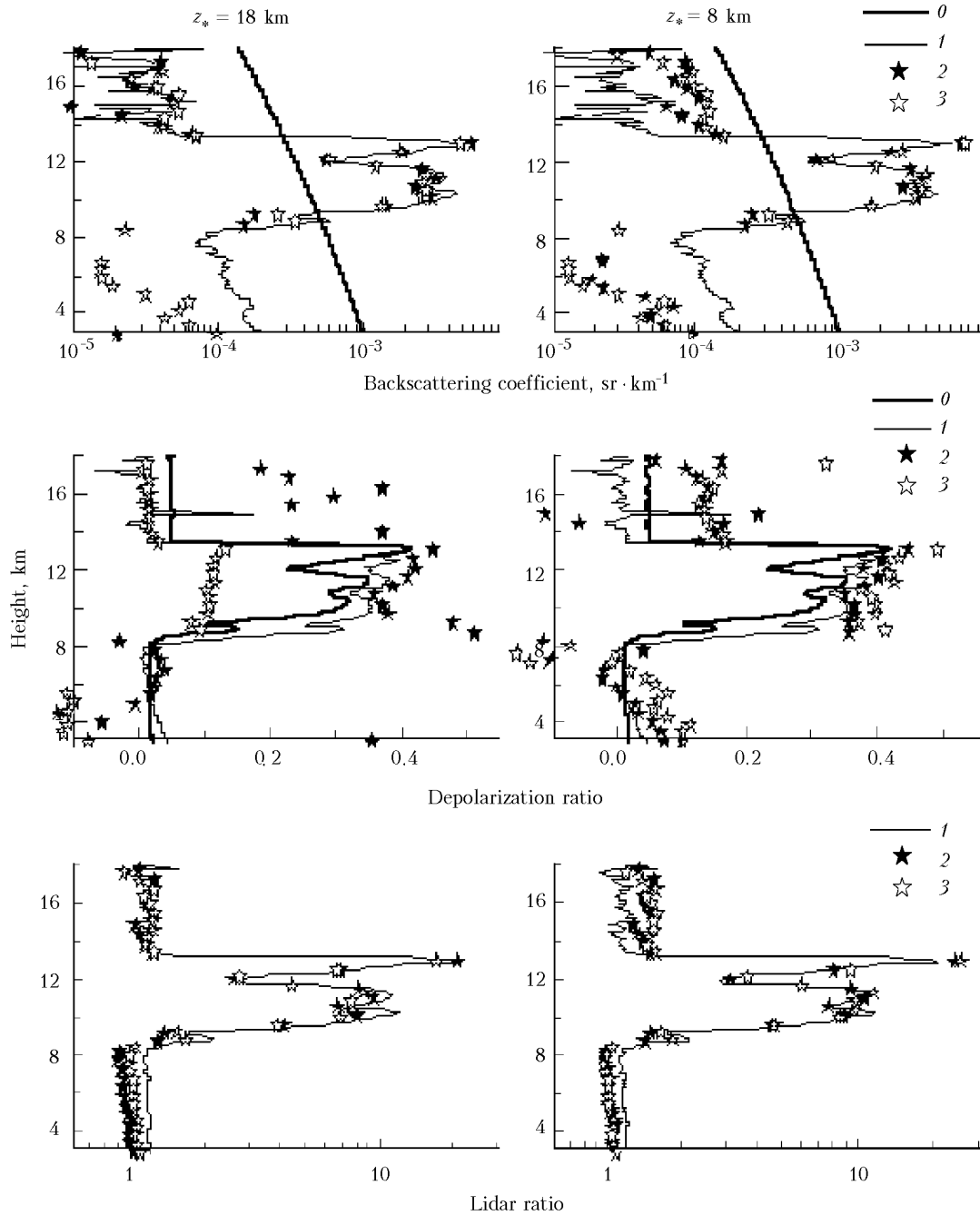

Fig. 3. Comparison of different methods for reconstruction of the optical parameters in the presence of the MS background ($\eta_1 = 0.5$, $\eta_2 = 0.6$). The structure of the figure and numeration of the curves are the same as in Fig. 1. No correction for the MS background was done.
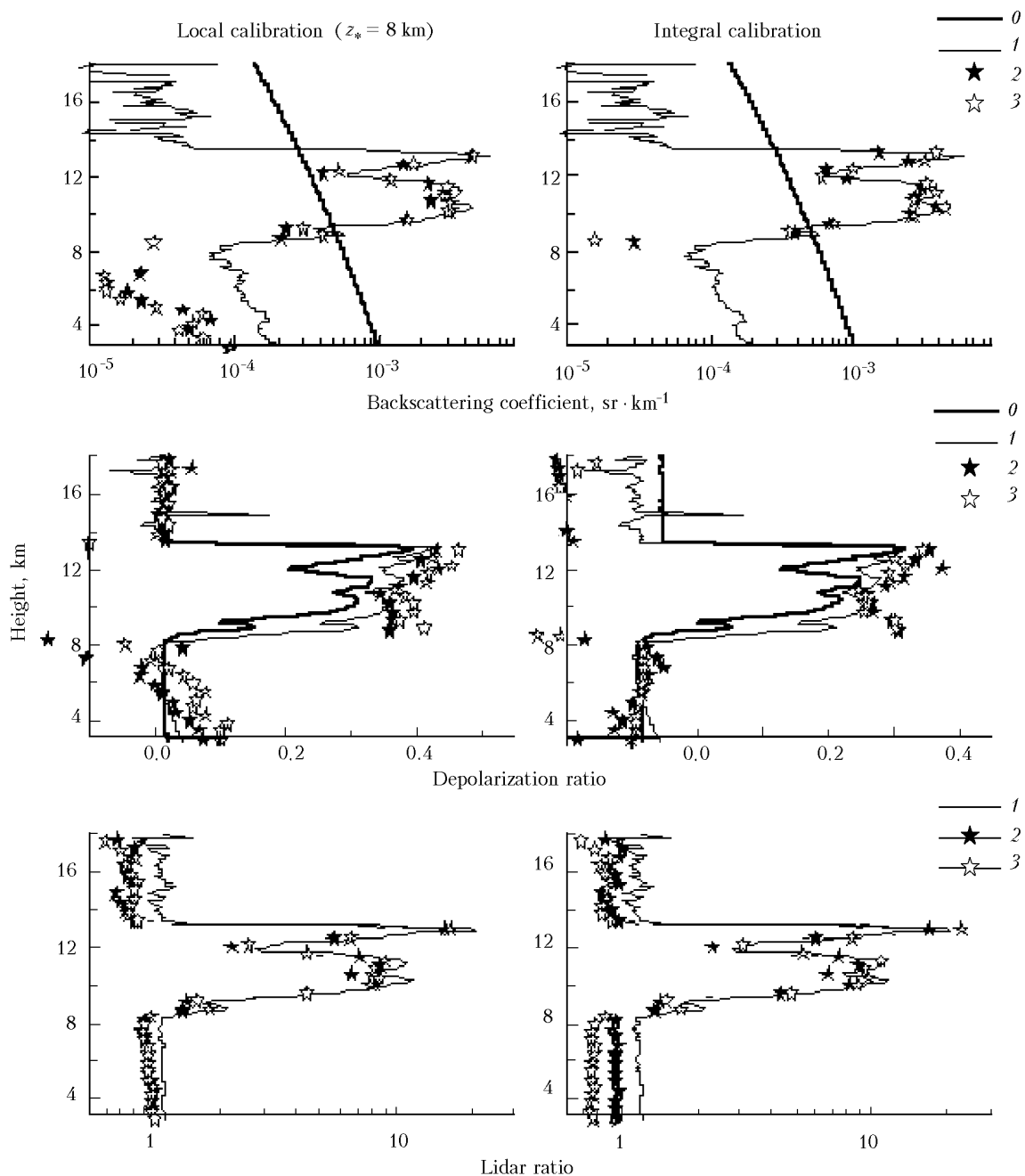
Fig. 4. The same as in Fig. 3, but with correction for the MS background. Left part of the figure is obtained at the local calibration at $z_* = 8$ km, the right part is obtained at estimation of $T_c^2(z_1, z_2)$ from the lidar returns according to Ref. 16.

Conclusion

Different methods for reconstruction of the optical parameters from the data of sounding by a polarization lidar are considered in the paper. The algorithm is proposed for reconstruction of the profiles of aerosol backscattering coefficient and depolarization ratio from the data obtained by a ground-based lidar, when the lidar signals in the majority of situations are described by the lidar equation in the single scattering approximation. The algorithm is applicable in the absence of data on the sensitivity ratio between the polarization channels. The methods of local and integral calibration are tested; the recommendations are done for the use of the methods under conditions of *a priori* uncertainty. The possible errors and the method for calibration in the presence of a significant MS background are studied.

S.V. Samoilova

Vol. 16, No. 10 /October 2003/ Atmos. Oceanic Opt. 835

References

1. K. Sassen, Bull. Am. Meteorol. Soc. **72**, 1848−1866 (1991).
2. V. Noel, H. Chepfer, G. Leganois, A. Delafal, and P.H. Flamant, Appl. Opt. **41**, No. 21, 4245−4257 (2002).
3. B.V. Kaul, S.N. Volkov, and I.V. Samokhvalov, Atmos. Oceanic. Opt. **16**, No. 4, 325−332 (2003).
4. S.R. Pal and A.I. Carswell, Appl. Opt. **24**, No. 21, 3464−3471 (1985).
5. O. Toon, E.V. Broweel, S. Kinne, and J. Jordan, Geophys. Res. Lett. **17**, 393−396 (1990).
6. B.V. Kaul, A.L. Kuznetsov, E.R. Polovtseva, and I.V. Samokhvalov, Atmos. Oceanic. Opt. **6**, No. 4, 257−261 (1993).
7. S.S. Khmelevtsov, Yu.G. Kaufman, V.A. Korshunov, E.D. Svetogorov, and A.S. Khmelevtsov, in: *Some Problems of Atmospheric Physics* (Gidrometeoizdat, St. Petersburg, 1998), pp. 358−393.
8. D. Deirmendjian, *Electromagnetic Scattering on Spherical Polydispersions* (American Elsevier, New York, 1969).
9. O.A. Volkovitskii, L.N. Pavlova, and A.G. Petrushin, *Optical Properties of Crystal Clouds* (Gidrometeoizdat, Leningrad, 1984), 198 pp.
10. F. Cairo, G.Di Donfrancesco, A. Adriani, L. Pulvirenti, and F. Fierli, Appl. Opt. **38**, No. 21, 4425−4432 (1999).
11. J.D. Klett, Appl. Opt. **24**, No. 11, 1638−1643 (1985).
12. F.G. Fernald, Appl. Opt. **23**, No. 5, 1609−1613 (1984).
13. A. Ansmann, M. Reibessel, and C. Weitcamp, Opt. Lett. **15**, No. 13, 746−748 (1990).
14. A. Ansmann, U. Wandinger, M. Reibessel, C. Weitcamp, and M. Michaelis, Appl. Opt. **31**, No. 33, 7113−7131 (1992).
15. S.V. Samoilova, Yu.S. Balin, and A.D. Ershov, Izv. Akad. Nauk SSSR, Fiz. Atmos. Okeana **39**, No. 3, 395−404 (2003).
16. S.A. Young, Appl. Opt. **34**, No. 30, 7019−7031 (1995).
17. A.D. Ershov, Yu.S. Balin, and S.V. Samoilova, Atmos. Oceanic Opt. **15**, No. 10, 810−815 (2002).
18. D.M. Winker, R.H. Couch, and M.P. McCormick, Proc. IEER, 164−180 (1996).
19. Yu.S. Balin, S.V. Samoilova, M.M. Krekova, and D.M. Winker, Appl. Opt. **38**, No. 30, 6365−6373 (1999).
20. V.A. Kovalev, Appl. Opt. **32**,No. 30, 6053−6065 (1993).
21. V.A. Kovalev, Appl. Opt. **42**, No. 3, 585−591 (2003).
22. C.M.R. Platt, J. Atmos. Sci. **30**, No. 6, 1191−1204 (1973).
23. C.M.R. Platt, J. Atmos. Sci. **38**, No. 1, 156−167 (1981).